Forest Ecology and Management 432 (2019) 264–275

Contents lists available at ScienceDirect

Forest Ecology and Management

journal homepage: www.elsevier.com/locate/foreco

A revised above-ground maximum biomass layer for the Australian continent

Stephen H. Roxburgh[a,*], Senani B. Karunaratne[b], Keryn I. Paul[a], Richard M. Lucas[c,g], John D. Armston[d,e,f], Jingyi Sun[g]

[a] CSIRO Land and Water, GPO Box 1700, Canberra, ACT 2601, Australia
[b] Department of the Environment and Energy, Parkes, ACT, Australia
[c] Department of Geography and Earth Sciences, Aberystwyth University, Aberystwyth, Ceredigion SY23 3DB, United Kingdom
[d] Department of Environment and Science Remote Sensing Centre, Ecosciences Precinct, Brisbane 4001, Queensland, Australia
[e] Joint Remote Sensing Research Program, School of Earth and Environmental Sciences, University of Queensland, St. Lucia, Brisbane 4067, Queensland, Australia
[f] Department of Geographical Sciences, University of Maryland, College Park, MD 20742, USA
[g] School of Biological, Earth and Environmental Sciences, The University of New South Wales, Sydney, NSW 2052, Australia

ARTICLE INFO

Keywords:
Forest biomass
Random forest
Carbon accounting
National greenhouse gas inventory

ABSTRACT

The carbon accounting model FullCAM is used in Australia's National Greenhous Gas Inventory to provide estimates of carbon stock changes and emissions in response to deforestation and afforestation/reforestation. FullCAM-predicted above-ground woody biomass is heavily influenced by the parameter *M*, which defines the maximum upper limit to biomass accumulation for any location within the Australian continent. In this study we update FullCAM's *M* spatial input layer through combining an extensive database of 5739 site-based records of above-ground biomass (AGB) with the Random Forest ensemble machine learning algorithm, with model predictions of AGB based on 23 environmental predictor covariates. A Monte-Carlo approach was used, allowing estimates of uncertainty to be calculated. Overall, the new biomass predictions for woodlands, with 20–50% canopy cover, were on average 49.5 ± 1.3 (s.d.) t DM ha^{-1}, and very similar to existing model predictions of 48.5 t DM ha^{-1}. This validates the original FullCAM model calibrations, which had a particular focus on accounting for greenhouse gas emissions in Australian woodlands. In contrast, the prediction of biomass of forests with a canopy cover > 50% increased significantly, from 172.1 t DM ha^{-1}, to 234.4 ± 5.1 t DM ha^{-1}. The change in forest biomass was most pronounced at sub-continental scales, with the largest increases in the states of Tasmania (166 to 351 ± 22 t DM ha^{-1}), Victoria (201 to 333 ± 14 t DM ha^{-1}), New South Wales (210 to 287 ± 9 t DM ha^{-1}), and Western Australia (103 to 264 ± 14 s.d. t DM ha^{-1}). Testing of model predictions against independent data from the savanna woodlands of northern Australia, and from the high biomass *Eucalyptus regnans* forests of Victoria, provided confidence in the predictions across a wide range of forest types and standing biomass. When applied to the Australian Government's National Inventory land clearing accounts there was an overall increase of 6% in continental emissions over the period 1970–2016. Greater changes were seen at sub-continental scales calculated within 6° × 4° analysis tiles, with differences in emissions varying from −21% to +35%. Further testing is required to assess the impacts on other land management activities covered by the National Inventory, such as reforestation; and at more local scales for sequestration projects that utilise FullCAM for determining abatement credits.

1. Introduction

FullCAM (Full Carbon Accounting Model) is a freely available software system for tracking greenhouse gas emissions and changes in carbon stocks associated with land use and management in Australian agricultural and forest systems (Richards, 2001; Richards and Brack, 2004; Richards and Evans, 2004; Brack et al., 2006; Waterworth et al., 2007). It is applied at the national scale for land sector greenhouse gas emissions accounting (Australian Government, 2018), and at the local scale for monitoring and reporting carbon sequestration projects, such as revegetation and the management of regrowth (Paul et al., 2015a,b).

FullCAM predicts the accumulation of above-ground biomass (AGB)

* Corresponding author.
E-mail address: stephen.roxburgh@csiro.au (S.H. Roxburgh).

https://doi.org/10.1016/j.foreco.2018.09.011
Received 8 August 2018; Received in revised form 7 September 2018; Accepted 9 September 2018
Available online 24 September 2018
0378-1127/

in woody vegetation using a hybrid of empirical and process-based modelling via the implementation of the Tree Yield Formula (TYF; Waterworth et al., 2007). The process-based modelling component utilises the forest growth model 3-PG (Landsberg and Waring, 1997) to derive a dimensionless index (the Forest Productivity Index, or FPI) that summarises potential site productivity for any given location based on the Normalised Difference Vegetation Index (NDVI), soil fertility, vapour pressure deficit, soil water content, and temperature (Kesteven and Landsburg, 2004). The empirical component is a statistical relationship between field-based observations of AGB (from minimally disturbed stands) and the FPI (Richards and Brack, 2004). This relationship is used to calculate the parameter M (the predicted maximum AGB for a given FPI), and is given by

$$M = (6.011 \times \sqrt{FPI} - 5.291)^2 \quad (1)$$

Parameter M is constant for any location in Australia, and is embedded within the FullCAM database as a spatial input layer with a resolution of 0.0025° (or approximately 250 m). Computationally, M exerts a strong influence on forest growth, affecting the rate of AGB accumulation, as well as defining the upper maximum biomass limit. M is also an important ecosystem property, with links to environmental productivity as well as a being a key indicator of ecosystem structure.

Over recent years evidence has accumulated that predictions of M for some vegetation types were biased, particularly for higher-biomass temperate forests, with lower M than observations would suggest (Montagu et al., 2003; Waterworth et al., 2007; Wood et al., 2008; Lowson, 2008; Keith et al., 2010; Roxburgh et al., 2010; Fensham et al., 2012; Preece et al., 2012). The presence of such bias may be due to the initial focus during FullCAM development on estimating carbon emissions and sequestration within Australia's woodland ecosystems, due to their ongoing active management. The forest types represented in the original field-based biomass estimates used in the relationship to predict M (Eq. (1)) had a strong representation of woodlands, but with < 10% of observations from higher-biomass (> 250 t DM ha^{-1}) temperate forests.

Since the development of FullCAM there has been a large increase in the availability of forest biomass data from across Australia, including from relatively undisturbed high biomass temperate forests. It was therefore timely to explore how these new data can be used to improve the estimation of M. The aim of this study was to use these new datasets to update FullCAM's M layer, and thus improve the accuracy of predictions of woody biomass growth for Australian woodlands and forests, and hence, Australia's National Greenhouse Gas Inventory.

2. Methods

Whilst it is possible to create *de novo* a new replacement biomass layer, by e.g. re-fitting the existing FPI vs observed biomass relationship on which the existing estimates of M are based (Eq. (1)), the approach adopted here was to update rather than replace the current M layer. This was to maintain continuity and consistency with the existing FullCAM modelling environment, and to allow new data to be applied only to regions with adequate data representation.

The detailed analysis steps are shown in Fig. 1, and can be summarised as follows:

1. Identify site biomass records that fulfil the criteria of being minimally disturbed, consistent with the definition of maximum biomass, M.
2. For each record i, calculate the ratio λ_i

$$\lambda_i = \frac{M_i}{O_i} \quad (2)$$

where M_i is the current prediction of maximum biomass (Equation (1)), and O_i is the field observation.

3. Use the Random Forest machine learning algorithm (Brieman 2001) to statistically model and predict λ across the continent, using a range of climatic and edaphic variables.
4. Update the existing M layer to M' by multiplying by the model-predicted λ

$$M' = \lambda M \quad (3)$$

2.1. Database of above-ground biomass observations

The primary source of AGB observation data was the TERN/Auscover National Biomass Library (NBL), available at http://www.auscover.org.au/purl/biomass-plot-library. This library is a collation of stem inventory and biomass estimates compiled from federal, state and local government departments, universities, private companies and other agencies. The biomass library contains (as of December 2017) 14,453 sites, 887,639 individual tree diameter measurements (> 5 cm), and 1467 species.

For inclusion in the analysis, the AGB estimates were required to represent predominantly mature and undisturbed vegetation (i.e. vegetation that has been minimally impacted by anthropogenic disturbances, and has not had a recent natural disturbance such as a wildfire or cyclone). Because not all sites within the NBL were located in vegetation that could be considered 'mature', it was first necessary to filter the database and exclude those observations that were most likely collected from disturbed vegetation. This was achieved by collating ancillary spatial datasets at both a national and state level that identified areas within which forests were more likely to be undisturbed (such as conservation lands), and also to identify areas where disturbance was more likely, for example areas subject to multiple use, including timber harvesting (Supplementary Data: Appendix A). Information was also gathered from the custodians of the NBL data where this indicated a measurement was located in disturbed or undisturbed (often referred to as remnant) vegetation. Records were also excluded if the observations were non-representative of the broader landscape, such as a number of Tasmanian records that specifically targeted forested areas with higher than average biomass (labelled 'LIMA' and 'LIMI' in the database; D. Mannes pers. comm.). A total of 5739 site records remained following this filtering (Table 1). To provide an additional check of the temporal continuity of forest cover, spatial forest cover mapping (> 20% cover) based on 25 Landsat images extending back to the 1970s were used to confirm woody vegetation cover over the period, thus indicating the absence of major disturbance (Australian Government 2018). Forest cover was defined as the mode within a 3 × 3 pixel window (approximately 75 m × 75 m) centred on the observation.

Preliminary analyses suggested improved empirical model performance could be obtained by stratifying the data and running separate statistical models based on two broad vegetation types corresponding to 'Forests' (with canopy cover > 50%) and 'Woodlands' (with canopy covers between 20 and 50%). The classification of sites within the database was based on forest and woodland cover as defined by the Australian National Forest Inventory (ABARES, 2014).

2.2. Vegetation classification for model prediction

Because M represents biomass at forest maturity, the spatial interpolation of the statistical models should represent the potential vegetation that an area could support, not the current vegetation distribution which reflects past land management, such as clearing of woody vegetation. The spatial interpolation was therefore based on the NVIS v4.2 1750 Major Vegetation Subgroups (MVS) classification (NVIS, 2016), which maps the extent of Australia's major vegetation types prior to extensive land clearing, at a 100 m resolution.

The NVIS subgroup for each of the 5739 records was extracted, and any subgroup that was represented by 50 observations or more was

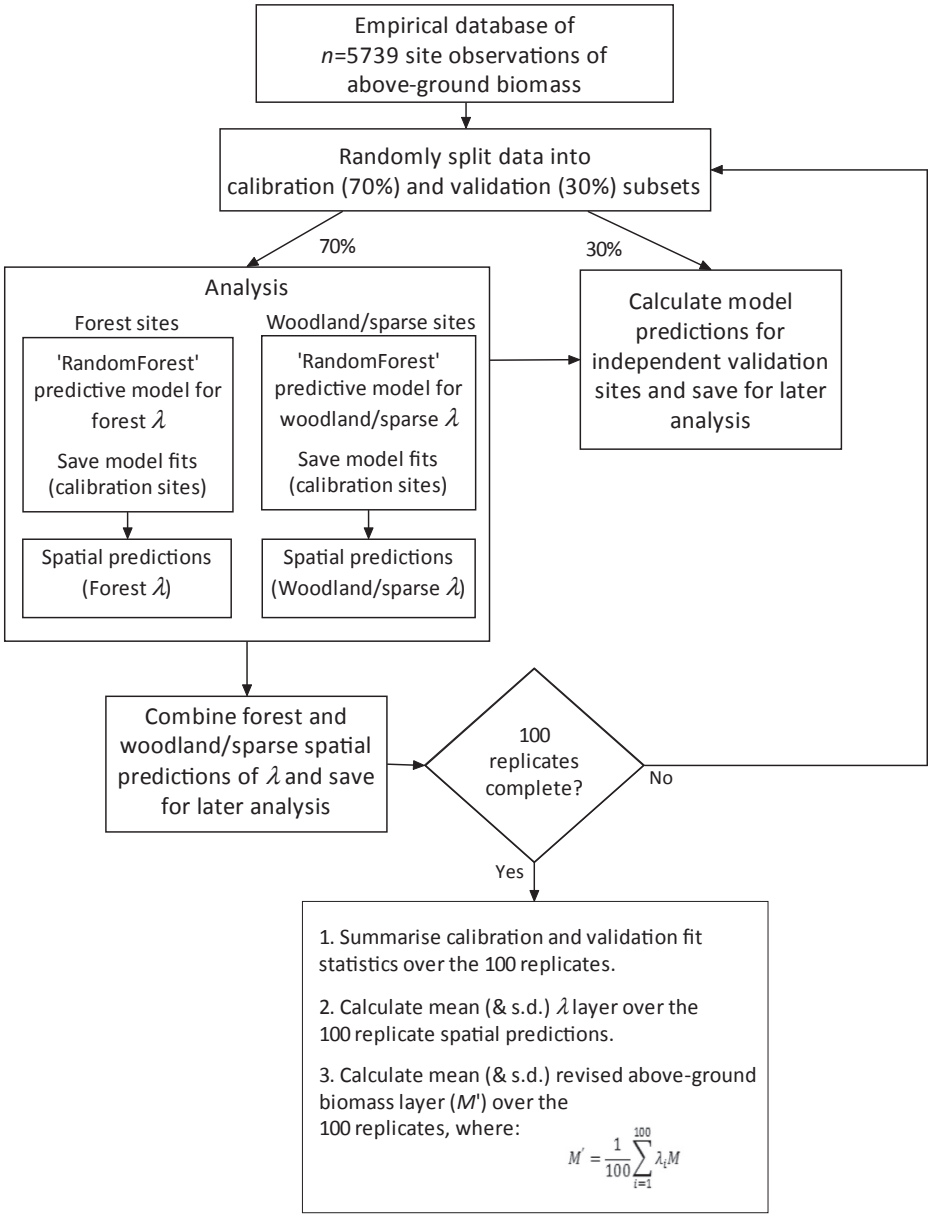

Fig. 1. Summary flowchart of analysis steps.

Table 1
Number of observations of above-ground biomass for each state and vegetation class.

	Forest	Woodland	Total
New South Wales	661	791	1452
Northern Territory	193	427	770
Queensland	604	2073	2262
Tasmania	920	66	986
Victoria	101	55	156
Western Australia	64	48	112
South Australia	0	1	1
Total	2543	3195	5739

included within the extent of the revised mapping calculation. The Forest and Woodland predictive models were applied on a subgroup-by-subgroup basis according to Table 2. In addition to the above criteria, data limitations restricted the extents of MVS classes 20, 27 and 45 (Table 2) to eastern Australia only (i.e. east of 132° longitude); and a small number of 'Forest' areas that fell outside the 600 mm annual rainfall isocline were reclassified as 'Woodland', recognising that arid 'forests' are closer to woodlands in terms of biomass and structure. Finally, a 3 × 3 majority smoothing filter was applied to the classification to remove isolated grid cells and gaps. The final extent (Fig. 2) defines the areas within which the existing *M* estimates were updated ('Included forests', and 'Included woodland'), and the areas with insufficient data and thus where the current *M* estimates were retained ('Excluded/non-woody').

2.3. Ensemble machine learning regression modelling with random forest

The analysis used a machine learning regression method to model, for each of the 5739 data points, the difference (or 'residual') between the current FullCAM estimates of *M*, and the NBL biomass estimates, defined as the ratio λ (Eq. (2)). Predictions of λ were then interpolated spatially and used to update *M* to *M′* (Eq. (3)).

The highly variable nature of the biomass data precluded the use of traditional statistical techniques, such as multiple regression, due to serious violation of the assumptions of normality and variance

Table 2
Primary classification of NVIS Major Vegetation System (MVS) vegetation classes into Forests (F) and Woodlands (W). Additional modifications to the primary classification are described in the text.

MVS Code	Forest Class	MVS Name
1	F	Cool temperate rainforest
2	F	Tropical or sub-tropical rainforest
3	F	Eucalyptus (± tall) open forest with a dense broad-leaved and/or tree-fern understorey (wet sclerophyll)
4	F	Eucalyptus open forests with a shrubby understorey
5	F	Eucalyptus open forests with a grassy understorey
6	F	Warm Temperate Rainforest
54	F	Eucalyptus tall open forest with a fine-leaved shrubby understorey
60	F	Eucalyptus tall open forests and open forests with ferns, herbs, sedges, rushes or wet tussock grasses
62	F	Dry rainforest or vine thickets
7	W	Tropical Eucalyptus forests and woodlands with a tall annual tussock grass understorey
8	W	Eucalyptus woodlands with a shrubby understorey
9	W	Eucalyptus woodlands with a tussock grass understorey
10	W	Eucalyptus woodlands with a hummock grass understorey
12	W	Callitris forests and woodlands
13	W	Brigalow (*Acacia harpophylla*) forests and woodlands
14	W	Other Acacia forests and woodlands
18	W	Eucalyptus low open woodlands with hummock grass
20	W	Mulga (*Acacia aneura*) woodlands and shrublands +/- tussock grass ± forbs
27	W	Mallee with hummock grass
45	W	Mulga (*Acacia aneura*) open woodlands and sparse shrublands ± tussock grass
47	W	Eucalyptus open woodlands with shrubby understorey
48	W	Eucalyptus open woodlands with a grassy understorey

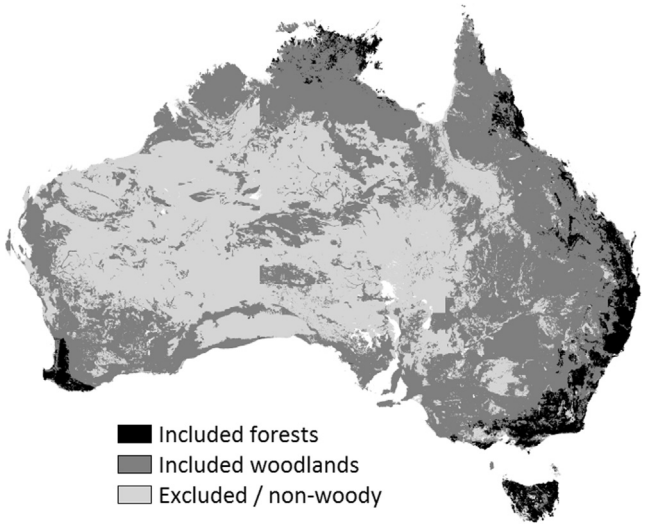

Fig. 2. Vegetation classification used to spatially map the separate Forest and Woodland predictive models for calculating the revised maximum biomass layer M′.

homogeneity. To overcome this, the Random Forest machine learning algorithm was used as the basis for prediction (Breiman, 2001). This method is based on random re-sampling of the data followed by the fitting of binary 'decision trees' that seek to minimise the error between observations and predictions. There were 23 predictor variables in the analysis (Table 3), comprising continental maps of soil carbon content (Viscarra Rossel et al., 2014), elevation (Jarvis et al., 2008), and 21 'WorldClim' v1.4 climate factors (Hijmans et al., 2005) obtained from the WorldClim database (http://www.worldclim.org). Continuous maps of predictor variables were required to allow spatial interpolation

Table 3
Independent variables used in the Random Forest ensemble machine learning regression modelling.

Variable	Description
Alt	Altitude (m a.s.l)
SOC	Soil organic carbon (t ha^{-1})
t_{max}	Mean monthly maximum temperature
t_{min}	Mean monthly minimum temperature
Bio_1	Annual Mean Temperature
Bio_2	Mean Diurnal Range (Mean of monthly (max temp − min temp))
Bio_3	Isothermality (BIO2/BIO7) (* 100)
Bio_4	Temperature Seasonality (standard deviation *100)
Bio_5	Max Temperature of Warmest Month
Bio_6	Min Temperature of Coldest Month
Bio_7	Temperature Annual Range (BIO5-BIO6)
Bio_8	Mean Temperature of Wettest Quarter
Bio_9	Mean Temperature of Driest Quarter
Bio_{10}	Mean Temperature of Warmest Quarter
Bio_{11}	Mean Temperature of Coldest Quarter
Bio_{12}	Annual Precipitation
Bio_{13}	Precipitation of Wettest Month
Bio_{14}	Precipitation of Driest Month
Bio_{15}	Precipitation Seasonality (Coefficient of Variation)
Bio_{16}	Precipitation of Wettest Quarter
Bio_{17}	Precipitation of Driest Quarter
Bio_{18}	Precipitation of Warmest Quarter
Bio_{19}	Precipitation of Coldest Quarter

of the resulting models. Latitude and longitude were also initially included as predictor variables to account for unexplained spatial variability, however they were excluded from the final analysis as they tended to lead to overfitting and the introduction of spatial artefacts. Model results were spatially interpolated using the 23 predictor variables at a resolution of 0.01°, or approximately 1 km. For reporting of spatial results, all layers were first transformed into Lamberts equal area projection prior to calculation.

Model fitting was based on 1000 Random Forest regression decision trees, with model predictions calculated as the median prediction over all 1000 trees (Meinshausen, 2006). As described in Section 2.1, initial exploration of the data indicated better model performance could be obtained by stratifying the data and running separate Random Forest models for the Woodland and Forest vegetation types.

A Monte-Carlo approach was used to assess the prediction error of the model fits, with the data randomly split into a 70% subset for model fitting, and a 30% subset that was excluded and retained for independent validation (Fig. 1). One hundred such data splits were made, with separate 'Forest' and 'Woodland' Random Forest models fitted to each of the 100 iterations, allowing the mean and standard deviation of results across the 100 replicates to be calculated. The data was randomly split by Constrained Latin Hypercube (Minasny and McBratney, 2006), to ensure representativeness across the predictor variable distributions between the calibration and the validation subsets.

For both the calibration and validation datasets four fit statistics were calculated, each summarising different aspects of the model performance. The first two summarise the main aspects of model accuracy; bias (quantified as Mean Absolute Error (*ME*)), and precision (quantified as the Root Mean Squared Error (*RMSE*)). In addition, model efficiency (EF, Nash and Sutcliffe, 1970) and Lin's concordance correlation coefficient (LCC, Lin, 2000) were calculated to provide overall assessments of model performance. EF is given by

$$EF = 1 - \frac{\sum_{i=1}^{n} (O_i - E_i)^2}{\sum_{i=1}^{n} (O_i - \overline{O})^2} \quad (4)$$

where O_i is the observed value of record i, E_i is the predicted value for record i, and $\overline{O}$ is the mean of the observations. A model efficiency of 1.0 indicates perfect prediction, and a value of 0.0 indicates the predictions are no better than the global mean of the observations. LCC is given by:

$$LCC = \frac{2S_{OE}^2}{S_O^2 + S_E^2 + (\overline{O}-\overline{E})^2} \quad (5)$$

where S_O^2 and S_E^2 are the variance of the observations and predictions respectively, S_{OE}^2 is the covariance, and $\overline{O}$ and $\overline{E}$ are the mean of the observations and predictions respectively. LCC is an index that measures the agreement between predictions and the 1:1 line, and is scaled between −1.0 and 1.0, with 1.0 indicating complete concordance.

2.4. Spatial autocorrelation

Because the NBL comprises a heterogeneous mixture of data collected at a range of spatial scales, a concern for the analysis was the clustering of sample points within close proximity to one another. Such clustering has the potential to invalidate the assumption of independence amongst observations, leading to bias in the predictor models. To address this the spatial correlation of sites was quantified, with the results suggesting minimal correlations (< 0.2) at distances between sites greater than approximately 10 km (Supplementary Data; Fig. A). To reduce the effects of spatial non-independence the data were first balanced prior to analysis through the method of bootstrap up-sampling (Kuhn et al., 2016), thus ensuring equality in the number of observations at the scale of 10 km × 10 km. Results from analyses conducted both with and without spatial up-sampling showed similar overall predictive performance, although with lower bias when the data were first spatially balanced.

All analyses were performed within the R statistical modelling environment (R Core Team, 2016). Random Forest model fitting was performed using the R library 'quantregForest' (Meinshausen, 2016); conditional latin hypercube sampling was performed using the 'cLHS' library (Roudier, 2011), and the 'caret' library function 'upSample' was used to spatially balance the data (Kuhn et al., 2016). All spatial mapping analyses were performed using the libraries 'raster' (Hijmans, 2016) and 'rgdal' (Bivand et al., 2016).

2.5. Model testing

In addition to the analysis of the hold-out validation records, that provide an internal estimate of the prediction error of the models when applied to new observations, the model predictions were also compared against two independent datasets that were not included in the analysis. In the first, predictions of *M′* were compared with the analysis of Cook et al. (2015), who estimated woody AGB for 23 biogeographic regions across northern Australia. This provided the opportunity to compare estimates of *M* and *M′* against an extensive set of biomass estimates for arid and savanna ecosystems. The second dataset comprised 78 observations of AGB in old-growth (≥250 year old) *Eucalyptus regnans* forests from the state of Victoria (Volkova et al., 2018). These forests are among the most biomass dense globally (Keith et al., 2009), and provide an opportunity to compare model predictions with independent observations collected within a forest type known to be under-predicted by the current estimates of *M*.

The Random Forest model predictions were also compared against other published modelled estimates of biomass for the Australian continent. Although this is a weaker test than comparing model predictions against empirical data, such cross-model comparisons are a useful tool for benchmarking, and for assessing overall congruence amongst different approaches. Four models were compared; the BiosEquil model of Raupach et al. (2001), the VAST 2.0 model of Barrett (2002), the TMSC model of Berry & Roderick (2006), and the BIOS2 model of Haverd et al. (2013). For these comparisons, where necessary total living biomass was converted to AGB assuming a root:shoot ratio of 0.25, and biomass carbon was transformed to dry mass by multiplying by 2.0.

Table 4
Fit statistics between observations (n = 5739) and model predictions for λ, and for the current (*M*) and revised (*M′*) estimates for maximum above-ground biomass.

Scope	*ME*	*RMSE*	*EF*	*LCC*
λ-Calibration	0.0	0.4	0.93	0.96
λ-Validation	−0.1	1.3	0.26	0.52
Original M	−35.3	239.1	0.14	0.25
M′-Calibration	−0.2	62.0	0.94	0.97
M′-Validation	−8.0	200.7	0.40	0.62

3. Results

3.1. Above-ground biomass database

Identifying biomass records that reflect potential maximum biomass, or biomass that has been minimally disturbed, is problematic given much of Australia is subject to regular disturbance such as fire, cyclones (in the far north), and with extensive anthropogenic modification such as clearing, grazing, timber harvesting and prescribed burning (Raison et al., 2003). The approach adopted here was to combine multiple lines of evidence to exclude sites most likely affected by prior disturbance, which included querying the source metadata and confirming with data custodians the status of particular records; the use of spatial data quantifying known disturbances such as harvesting; the use of tenure maps to identify areas least likely to be subject to anthropogenic disturbance; and use of the historical satellite record to confirm continuity of vegetation cover over time. We note that none of these methods are perfect, and that the theoretical ideal of vegetation at maximum biomass is likely very rarely, if ever, met in reality. The result of the above filtering was a reduction of the initial records by approximately 60%, from 14,453 to 5739.

For the development of the existing *M* layer, Richards and Brack (2004) determined forest stand age from disturbances detected from 12 Landsat remotely sensed coverages collected between 1972 and 2002. A similar analysis conducted here, based on 25 coverages spanning the period 1972 to 2016, showed over 90% of records were classified as forest cover for > 20/25 of the annual coverages, with over 75% showing continuous forest cover (Supplementary Data; Fig. B). Given the majority (> 70%) of records that showed intermittent forest cover were located in woodlands rather than forests, changes in cover classification are likely due to temporal variability in woodland tree canopy cover. Uncertainty in the geo-locations of the records and/or variability in satellite image quality may also contribute to this variability, although the forest cover detection based on a 3 × 3 window around the target locations was designed to minimise such errors.

3.2. Random forest model performance

The Random Forest model fit statistics, for both calibration (when the records were used as part of model fitting) and validation (when records were withheld from model fitting) were based on comparisons between observed biomass, and model predictions for each record. For calibration, estimates for each record were based on the average over the approximately 70/100 replicates where each site was used for fitting; and for validation the average of the approximately 30/100 replicates where each site was withheld from fitting. An alternative analyses where a single Random Forest run utilising all 5739 records and using the internally calculated out-of-bag (OOB) estimates for validation yielded almost identical results; however the Monte-Carlo approach adopted here additionally allowed spatial maps of uncertainty for the predicted *M′* layer to be readily calculated.

The overall predictions of λ when records were used for model calibration were unbiased (*ME* = 0.0), with a *RMSE* of 0.4 and high

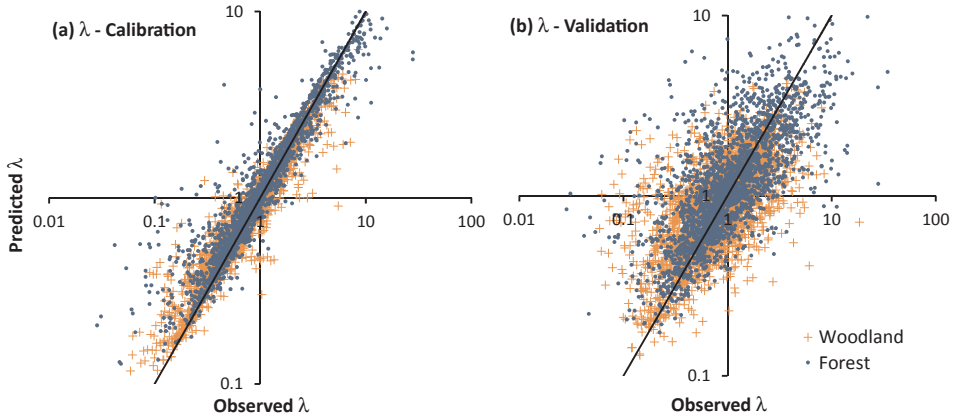

Fig. 3. Observed vs. Random Forest model-predicted λ for (a) the 5739 data points when utilised for model calibration; and (b) the 5739 data points when withheld for independent validation. Fit statistics are given in Table 4.

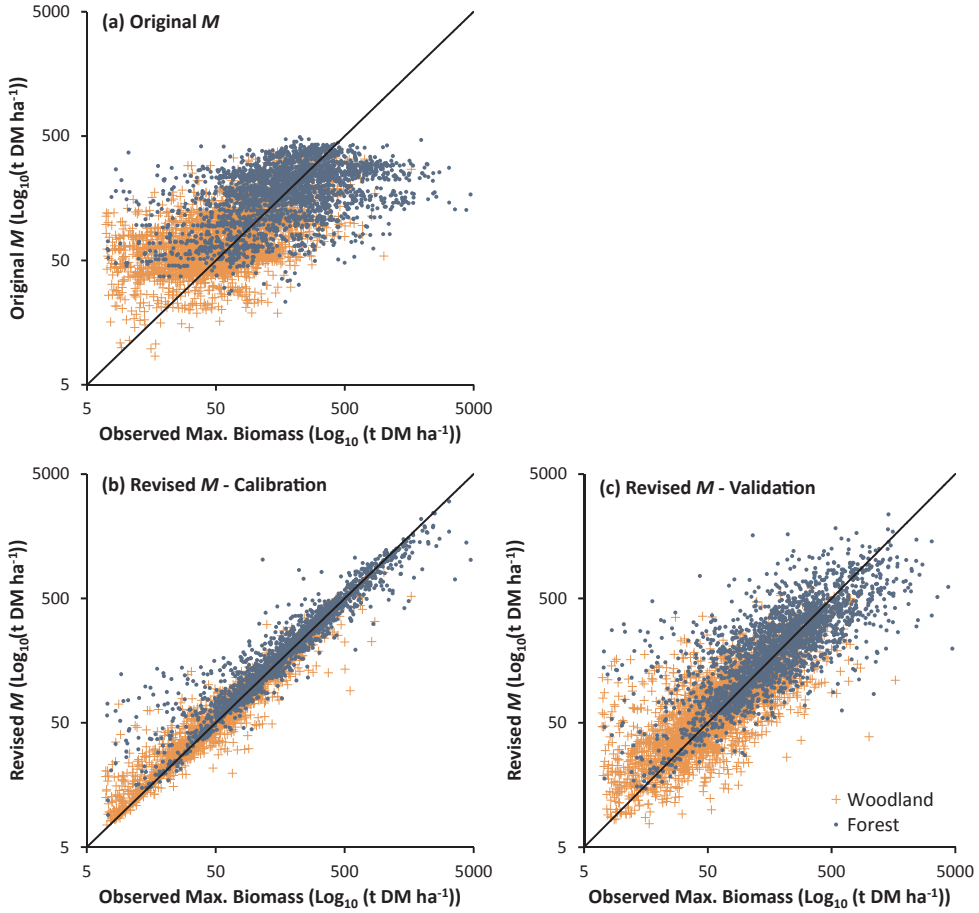

Fig. 4. Observed vs. Predicted above-ground biomass for each of the 5739 data points, for (a) the original FullCAM *M* estimates; and (b) and (c) the revised estimates *M′* for the calibration and validation results through application of the modifier λ. Fit statistics are given in Table 4.

values of *EF* (0.93) and *LCC* (0.96) (Table 4), thus indicating strong overall agreement between observations and predictions (Fig. 3a). When records were used for validation there was evidence for some bias (*ME* = 0.1) with lower precision, and correspondingly lower values for *EF* and *LCC* (Table 4; Fig. 3b). Note for purposes of display the axes in Figs. 3 and 4 are logarithmically transformed, but all model fitting and the calculation of the fit statistics was based on untransformed data.

The fit statistics were also calculated for the final predicted maximum biomass estimate, *M′* (Eq. (3)). This has the additional advantage of allowing equivalent statistics to be calculated for the current *M* layer. Comparison of the current *M* estimates with the observations shows an overall bias (under-prediction) of −35.3 t DM ha^{-1}, with a *RMSE* of 239.1 t DM ha^{-1}, and with low indices for the statistics quantifying overall fit (*EF* = 0.14; *LCC* = 0.25) (Table 4). This is reflected in the scatter of observed vs predicted biomass (Fig. 4a), where the bias is particularly apparent for high biomass observations, with observations > 500 t DM ha^{-1} all predicted to be lower than 500 DM ha^{-1} (Fig. 4a). In contrast, the revised *M′* modelled estimates for the calibration analysis are effectively unbiased (*ME* = −0.2 t DM ha^{-1}), and the *RMSE* has approximately quartered, from 239 t DM ha^{-1} down to

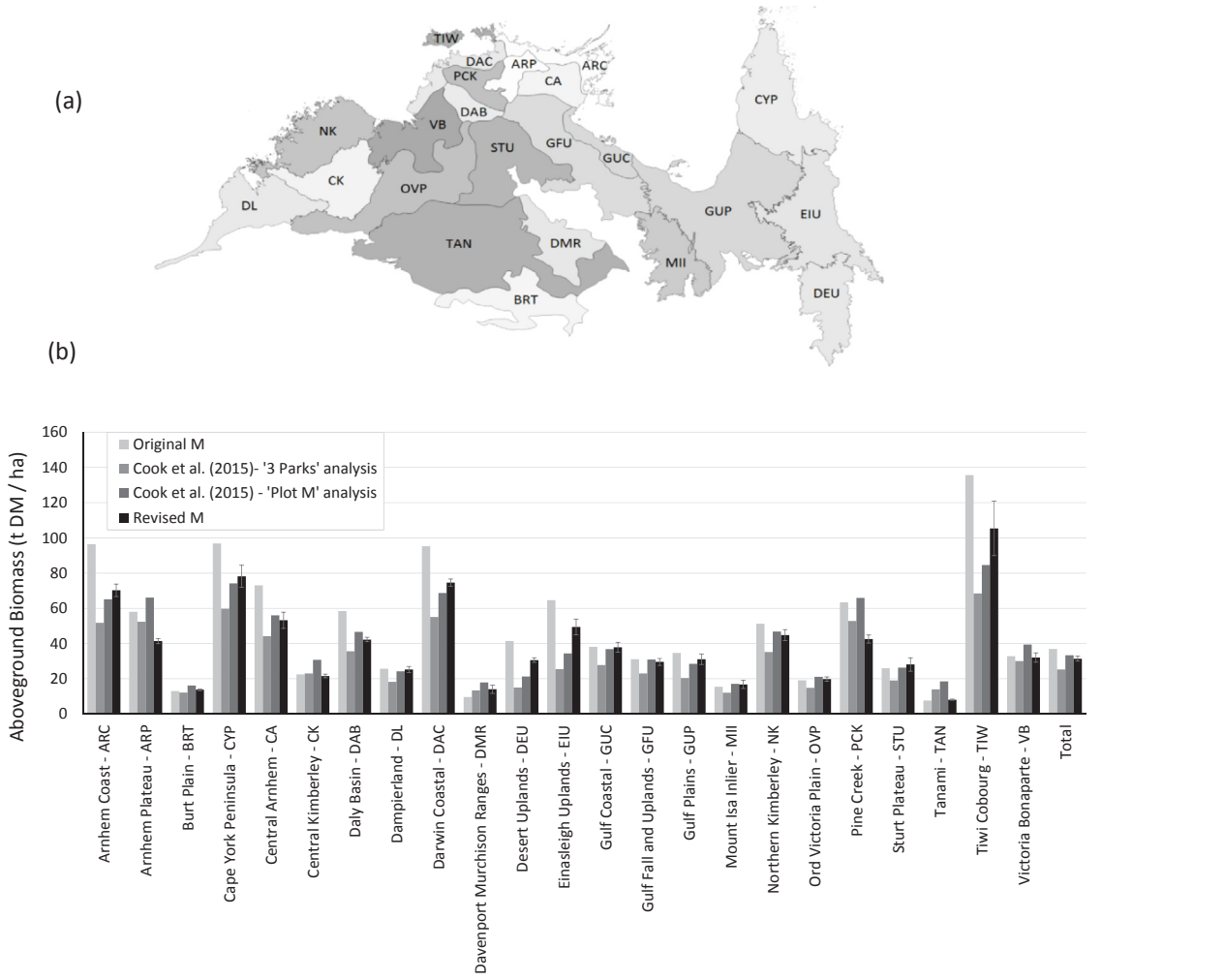

Fig. 5. Comparison of the original and revised maximum above-ground biomass with the independent analysis of Cook et al. (2015). (a) the IBRA regions of Northern Australia (b). Aboveground biomass estimates for each IBRA region.

62 t DM ha^{-1}, with correspondingly high values for *EF* (0.94) and *LCC* (0.97) (Table 4). When applied to the validation data, there was evidence for a bias of −8 t DM ha^{-1}, and a corresponding reduction in precision, with a *RMSE* of 200 t DM ha^{-1}. At the continental scale, this bias equates to an error of approximately 5% under-prediction.

Of the 23 predictor variables, soil organic carbon was the most important explanatory variable for the Woodlands model, and precipitation of the driest month for the forest model (Supplementary data; Fig. C). Variable importance was quantified as the percent increase in the model fit error following the removal of the target variable.

3.3. Model testing against independent data

For much of northern Australia the revised estimates of maximum biomass (*M′*) were lower than predicted by the current *M* (Fig. 5). This reduction is consistent with the data of Cook et al. (2015), that also showed generally lower biomass compared with existing *M*. Overall, the estimates of revised *M′* are now closer to the values reported by Cook et al. (2015), with the average of the revised estimate (31 ± 1 t DM ha^{-1}) falling between the estimates based on the two calculation methods of Cook et al. (2015) (25–33 t DM ha^{-1}). This contrasts with the current *M* estimate of 37 t DM ha^{-1}. At the scale of individual analysis regions there were some discrepancies, with *M′* predictions ranging from −57% to 43% of observations, depending on the region (Fig. 5b).

For the high biomass *Eucalyptus regnans* forests of Victoria the current mean biomass predicted by *M* is 266 t DM ha^{-1} (and never predicted to exceed 500 t DM ha^{-1}), with a relatively narrow range of values and a large peak in the frequency distribution in the 250–350 t DM ha^{-1} class (Fig. 6b). This is well below the observed biomass, with a mean of 886 t DM ha^{-1}, and with some individual observations exceeding 1500 t DM ha^{-1}. The revised *M′* estimates show a frequency distribution that has shifted to overlap with those of the observations, with the mean biomass increasing from 266 t DM ha^{-1} to 656 t DM ha^{-1}, and with predictions up to 1500 t DM ha^{-1} (Fig. 6). Although the frequency distribution of *M* and *M′* closely align up to approximately 1200 t DM ha^{-1} (Kolmogorov-Smirnoff test: $P = 0.061$), across the full range of site biomass there are significantly fewer very high biomass records than observed (Kolmogorov-Smirnoff test: $P < 0.001$).

When compared against four alternative continental-scale modelled estimates of biomass, *M′* was within the reported range for the broad forest and woodland vegetation classes depicted in Fig. 4 (Table 5). The mean *M′* continental Forest biomass of 234 t DM ha^{-1} compares with 210–278 t DM ha^{-1} across the four models, and the mean woodland estimate of 50 t DM ha^{-1} compares with 49–54 t DM ha^{-1}.

3.4. Spatial prediction of above-ground biomass

A comparison of the original above-ground biomass layer (*M*, Fig. 7a) with the revised layer (*M′*, Fig. 7c) shows the major differences to be in the temperate forest ecosystems, particularly in Western Australia, Eastern Tasmania, Victoria and New South Wales where there

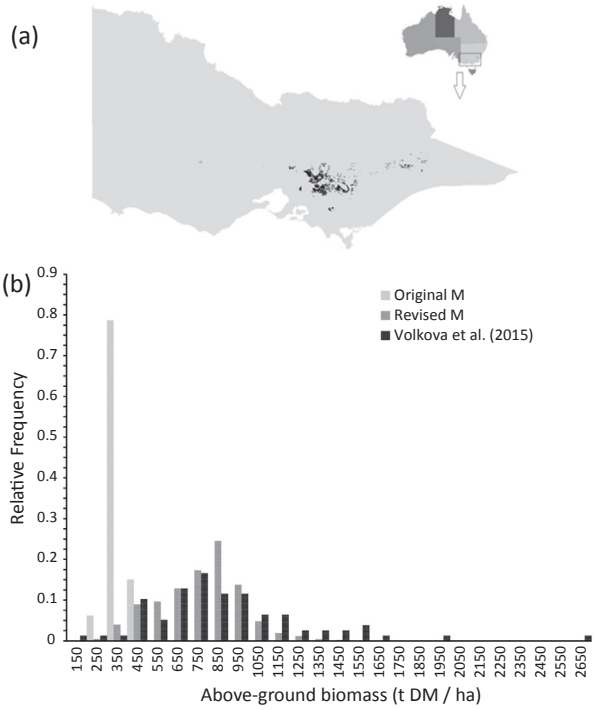

Fig. 6. Comparison of the original and revised maximum above-ground biomass with the independent observational database of Volkova et al. (2018), of $n = 78$ old-growth (≥250 year old) *Eucalyptus regnans* forest biomass sites in the Central Highlands area of Victoria. (a) Location map showing the distribution of *Eucalyptus regnans* in the central highlands region of Victoria. (b) Relative frequency distribution of biomass for the 78 old-growth observations, and for the original and revised model predictions of *M*.

Table 5
Predicted above-ground biomass (t DM ha^{-1}) from four continental-scale models, and the estimates for *M* and *M′*. Values in parentheses for *M′* are the standard deviations over 100 replicate analyses. No 'Excluded/non-woody' value is given for *M′*, as the current *M* values are assumed for those areas.

	M	*M′*	BIOS2[1]	TMS[2]	VAST 2.0[3]	BiosEquil[4]
Forest	172.1	234.4 (5.1)	209.7	217.5	221.3	278.2
Woodland	48.5	49.5 (1.3)	52.1	53.9	49.3	50.2
Excluded/non-woody	16.1	–	17.0	11.2	13.8	14.5

[1] Haverd et al. (2013).
[2] Berry & Roderick (2006).
[3] Barrett (2002).
[4] Raupach et al. (2001).

have been significant increases in predicted AGB. Areas where *M′* has declined relative to *M* include much of northern Australia and far north Queensland (Fig. 7b; see also Fig. 5).

These trends are more apparent when summarised on a state-by-state basis, either through comparison of the mean biomass across the 5739 records used in the analysis, which shows *M*, *M′*, as well as the field observations (Fig. 8), or through comparison when averaged spatially (Fig. 9).

At the continental scale there was a slight bias in the predictions of the independent validation subset of the data, in the order of 5% under-prediction, driven by the higher-biomass 'forests' (Fig. 8a). Overall, there was a significant improvement in the agreement between the model predictions and the observations compared to the current *M* estimates.

4. Discussion

Woody biomass growth within FullCAM is strongly influenced by the parameter *M*, which defines the maximum upper limit to biomass accumulation at a given location. As noted in the introduction several analyses have suggested *M* currently under-predicts biomass in some forest types, particularly temperate forests. For example, Waterworth et al. (2007) had to apply growth modifiers to increase the biomass predictions of FullCAM for plantation forests. Similarly, for mallee and environmental plantings Paul et al. (2015a, 2015b) addressed FullCAM's biomass under-prediction through modifying FullCAM parameters other than *M* directly. Here we provide a more general solution by developing an updated biomass layer, *M'*, that can be applied to any location within Australia.

Overall, the Random Forest statistical modelling and the resulting updated biomass layer *M′* improved the current maximum biomass predictions, with bias at the continental scale reducing from −35 t DM ha^{-1} down to negligible levels for the fitted model, and down to −8.0 t DM ha^{-1} (or approximately 5% error on average) when the model is applied operationally to new data (Table 4). The source of this remaining bias is uncertain, but is possibly due to over-fitting of the Random Forest algorithm to the calibration data. Precision in the biomass predictions improved from 239 t DM ha^{-1} down to 62 t DM ha^{-1} for the calibration data, and down to 201 t DM ha^{-1} when applied to new data (Table 4). The improvements in model prediction were particularly marked for forests with AGB biomass > 500 t DM ha^{-1}.

At the continental scale, and for the lower-biomass woodland vegetation with a canopy cover 20–50%, there were minimal differences in predicted biomass between the new *M′* (49.5 ± 1.3 t DM ha^{-1}, mean and s.d.) and the existing *M* (48.5 t DM ha^{-1}) (Fig. 9a). This provides strong support for the original FullCAM calibrations, where the focus was primarily on woodland ecosystems due to their active management, and thus importance for national greenhouse gas accounting. In contrast, predictions of forest biomass (with canopy cover > 50%) greatly increased between *M* and *M′*, from a continental average of 172 t DM ha^{-1} to 234 ± 5.1 t DM ha^{-1} (Fig. 9a). For individual states, increases in predicted maximum forest biomass were typically much greater; the original *M* for Western Australia was 103 t DM ha^{-1}, compared with 264 ± 14 t DM ha^{-1} under the revised analysis. Similar increases were found for Tasmania (166 to 351 ± 22 t DM ha^{-1}), Victoria (201 to 333 ± 14 t DM ha^{-1}) and New South Wales (210 to 287 ± 9 t DM ha^{-1}).

When compared against AGB predictions from four independent continental-scale models, the *M′* estimates for all vegetation classes (forest, woodland and excluded/non-woody) fell within the range of the published models (Table 5), noting that forests with a canopy cover > 50% were initially outside of the range prior to updating (172.1 t DM ha^{-1}, compared to model predictions of 210–278 t DM ha^{-1}).

The new *M′* biomass predictions also compared favourably when tested against independent data not included in the modelling procedure. For Northern Australia the decline in predicted biomass from the current *M* estimates (37 t DM ha^{-1}) to *M′* (31 ± 1 t DM ha^{-1}) is consistent with the analysis of Cook et al. (2015), who gave an overall estimate of 25–33 t DM ha^{-1}. The upper estimate of Cook et al. (2015) is based on an assumed stem diameter distribution that is representative of a more mature forest structure (their 'Plot M' analysis), and is thus likely to be closer to the assumed minimal disturbance assumption of the *M* parameter.

For the old-growth high biomass *Eucalyptus regnans* forests of Victoria the average AGB across the field observations was 886 t DM ha^{-1}, which is similar to the heartwood-decay adjusted estimate of Sillett et al. (2015) of 935 t DM ha^{-1} and the catchment-scale mean of 1002 t DM ha^{-1} of Keith et al. (2009), and is within the range reported by Dean et al. (2012) for the same forest type (840–1305 t DM ha^{-1}, varying by site index). The revised *M′* estimate increased the mean

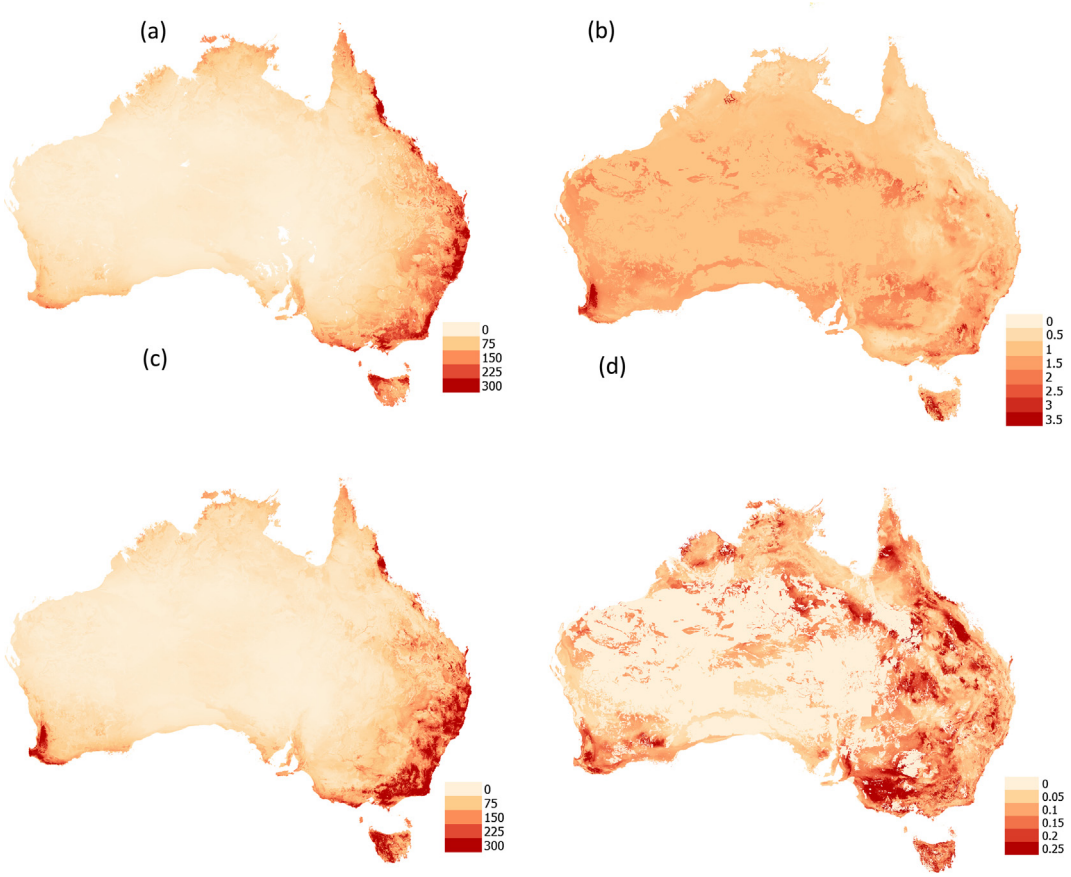

Fig. 7. (a) Original FullCAM maximum biomass layer (*M*, t DM ha^{-1}). (b) Maximum biomass modifier layer (λ) predicted from the Random Forest model (dimensionless multiplier). (c) Revised maximum biomass layer, calculated from a x b (*M′*, t DM ha^{-1}). (d) Coefficient of variation (standard deviation/mean) of *M′*, calculated over 100 Random Forest model fits.

predicted biomass of the *E. regnans* from 266 to 656 ± 31 t DM ha^{-1}, with a spatial distribution of values that shifted to be broadly consistent with the observations, though with a tendency to under-predict the highest biomass locations in the landscape (Fig. 6b). This under-estimation likely results from the constraints imposed by simultaneously optimising all possible forest types within Australia. Higher accuracy at the local scale could be achieved by further sub-dividing the forest and woodland classes, though data limitations for many vegetation types would be a barrier to the general application of such an approach.

In a study concentrating solely on the forests south-east Australia, Keith et al. (2010) predicted a mean maximum AGB of approximately 434 t DM ha^{-1}, which is 28% higher than the 313 t DM ha^{-1} predicted by *M′* for the combined forests of Tasmania, Victoria and New South Wales. Keith et al. (2010) discuss a number of sources of uncertainty that could potentially contribute to such a discrepancy, such as differences in the allometric models applied to estimate field biomass, the extent to which field data are representative of the diversity across the landscape, and the methods used to spatially extrapolate the data. An additional contributing factor could be differences in the spatial extents of the two studies. Given the broad scope of the NBL and the wide range of contributing data sources, it is also likely that residual impacts of historical anthropogenic disturbance are present in some of the records, which would tend to make our estimates conservative.

FullCAM is primarily used for calculating greenhouse gas emissions from the land sector as part of national greenhouse gas reporting requirements (Australian Government, 2018). Within this context, a thorough investigation of the impacts of updating the maximum biomass layer can only be made by embedding *M′* within the FullCAM simulation environment, and running simulations that include not only the growth of AGB, but also the flow-on effects to the allocation of this new growth to stems, branches, bark, leaves and roots, and ultimately to the influence of clearing, harvesting or fire events on carbon pool dynamics, and the production and decay of debris and soil organic carbon. An initial investigation of the potential implications for changes in net ecosystem emissions between *M* and *M′* resulting from deforestation and subsequent regrowth over the period 1970–2016 showed an increase in emissions, at the continental scale, of 6%. However, at a regional level, with emissions reported within 6° × 4° analysis tiles, the differences ranged from a 35% increase in emissions (south-west Western Australia) to a 21% decrease (central-east Queensland). The overall low impact of the updated *M′* at the continental scale is because most of the land clearing in Australia since 1970 has occurred in woodland ecosystems, and these systems showed little overall change between *M* and *M′*. Much larger differences would be expected in areas of reforestation of higher-biomass forests, or when accounts are calculated in the higher biomass forests of Australia.

Applying the concept of maximum potential biomass is problematic for many Australian ecosystems due to the ubiquitous occurrence of fire and other disturbances that can lead to mortality and the reduction of living biomass (Raison et al., 2003). This makes it difficult to identify and validate site-based data that has been minimally disturbed; and when undisturbed areas are identified there may be questions over how well they represent the broader landscape, particularly when they occur as remnant patches. Here we used a combination of different lines of evidence to filter the available database to exclude sites that were likely to have been recently disturbed. Ideally, sites would be individually investigated in detail to confirm their status, such as done by Raison et al. (2003) for the initial FullCAM calibrations. However, with over 14,000 site estimates currently available such detailed site-by-site investigations are impractical. There is thus a trade-off between including

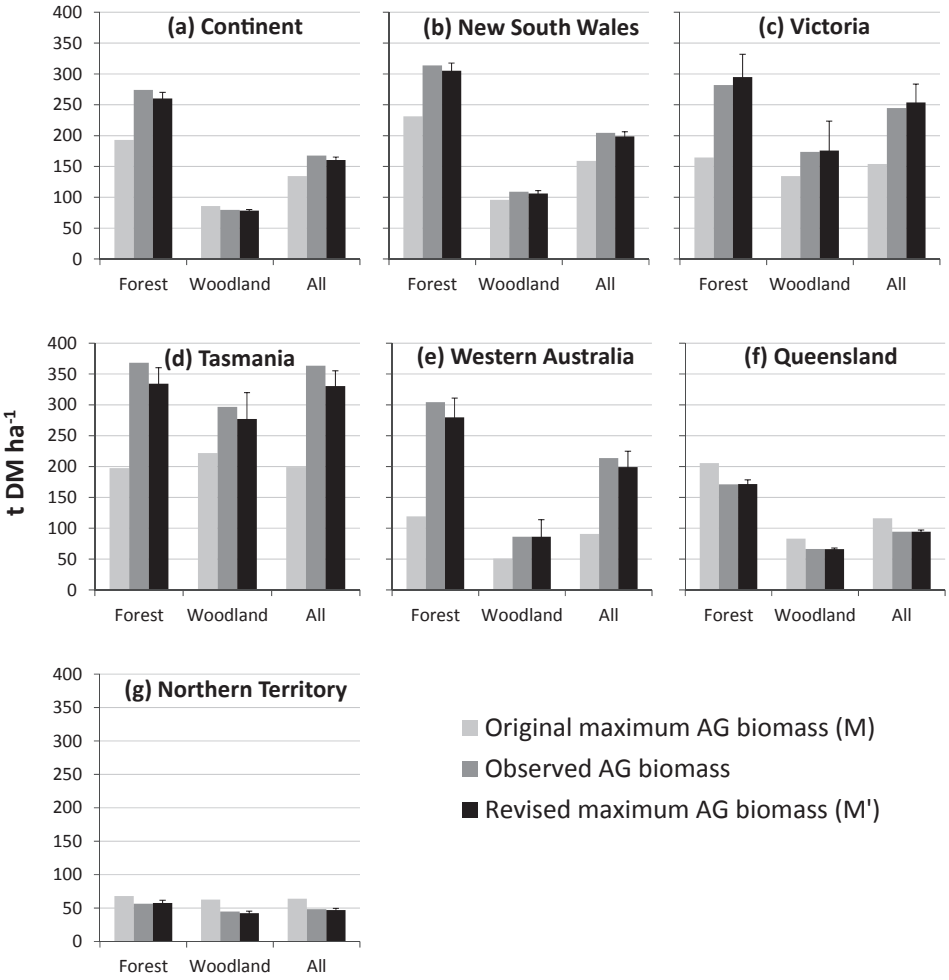

Fig. 8. Comparison of the mean above-ground biomass across the 5739 observed data points with the mean biomass from the original (*M*) and revised (*M′*) predictions of above-ground biomass. South Australia is excluded due to lack of data. The number of observations for each state x vegetation type combination are given in Table 1.

a small number of sites where the site history has been researched in detail, with the associated risk that they may be non-representative at the continental scale, and the inclusion of a broader sample such as adopted here, with the risk that some sites included for analysis may have been subject to historical disturbance, either natural or anthropogenic. The general agreement between the independent data of Cook et al. (2015) and Volkova et al. (2018) and *M′* give us confidence that gross errors of classification have been avoided, but an extra layer of detailed checking, for example on a random subset of the 14,000 available records, would provide additional confidence in the results.

Whilst the revised *M′* was applicable to approximately 54% of the continent covered by woodlands and forests (Fig. 2), there was insufficient data to adequately assess the current performance of *M* for the most arid regions, which includes large areas of the Australian rangelands, such as the hummock grasslands, and the mulga woodlands in the western half of the continent. The collation and assimilation of rangelands data, similar to the development of the NBL for woodlands and forests, would allow the analysis described here to be extended into these lower-biomass systems. Such an activity would provide additional support and confidence for the development of methods for managing rangelands for improved greenhouse gas outcomes.

Further assessment of the implications of *M′* when embedded within the FullCAM software environment are required. Although application to the deforestation account within the national greenhouse gas accounting system showed minimal impacts at the continental scale, this was due to minimal changes between *M* and *M′* for the woodland systems within which most clearing and regrowth activity has taken place. The next steps for testing include similar analyses for other areas of the national accounts, such as reforestation and the sequestration/emissions associated with environmental plantings, and perform model re-calibration as necessary. We further note that operationalising *M′* within the current FullCAM system has implications for vegetation that has already undergone separate calibration, such as mallee and environmental plantings. For such cases additional modifications to the FullCAM system will be required to avoid issues of 'double calibration'. Further work is also required to investigate the potential impacts of updating *M* on those project activities under the Australian government's Emissions Reduction Fund (ERF, Australian Government, 2014) that use FullCAM for calculating sequestration credits. This will particularly involve activities associated with avoided deforestation, and the management of regrowth.

5. Conclusions

Maximum above-ground biomass (*M*) is a key parameter in the Australian Government's land sector greenhouse gas accounting tool, FullCAM, affecting both the maximum biomass attainable by the model, and the rate of forest growth. *M* is also an important ecosystem property, with links to environmental productivity as well as being a key indicator of ecosystem structure. Here we updated the current FullCAM *M* layer through combining an extensive database of 5739 site-based estimates of forest and woodland biomass with the Random Forest

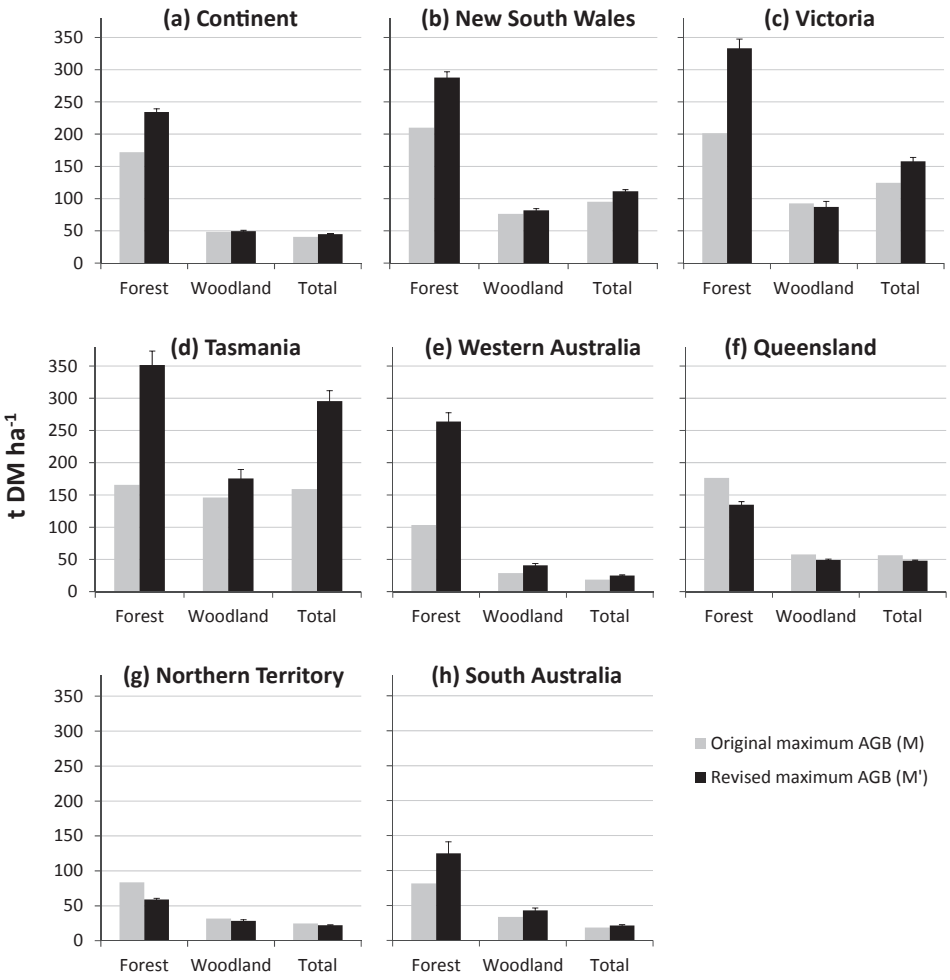

Fig. 9. Comparison of the spatially-averaged above-ground biomass for the original predictions (*M*) and the revised predictions (*M'*).

ensemble machine learning algorithm. Key improvements were in the prediction of temperate forest biomass, with biomass increasing continentally from 172.1 t DM ha^{-1} to 234.4 ± 5.1 t DM ha^{-1}, and with significant improvements in biomass prediction at sub-continental scales (Tasmania: 166 to 351 ± 22 t DM ha^{-1}; Victoria: 201 to 333 ± 14 t DM ha^{-1}; New South Wales: 210 to 287 ± 9 t DM ha$^{-1;}$ and Western Australia: 103 to 264 ± 14 s.d. t DM ha^{-1}). In contrast, the biomass of lower productivity woodlands remained largely unchanged, from 48.5 t DM ha^{-1} to 49.5 ± 1.3 t DM ha^{-1}, thus validating the original FullCAM model calibrations which had a particular focus on accounting for greenhouse gas emissions in Australian woodlands. Comparison against independent datasets provided confidence in the model predictions across a wide range of forest types and standing biomass. Initial investigations into the implications of the new *M* layer for Australia's national greenhouse gas accounts are reported.

Acknowledgements

This work was funded in part by the Australian Government through The Department of the Environment and Energy. We thank Trevor Booth and Stephen Stewart for providing constructive criticism on a draft of the manuscript. Senani B. Karunaratne wishes to clarify that the views and opinions expressed in this research work do not necessarily reflect those of the Australian Government or the Minister for the Department of the Environment and Energy.

Appendix A. Supplementary material

Supplementary data to this article can be found online at https://doi.org/10.1016/j.foreco.2018.09.011.

References

ABARES, 2014. Forests of Australia (2013), Australian Bureau of Agricultural and Resource Economics and Sciences, Canberra, available at http://data.daff.gov.au/anrdl/metadata_files/pb_foa13g9abfs20140604_11a.xml.

Australian Government, 2014. Emissions Reduction Fund White Paper, Commonwealth of Australia, Canberra, available from: https://www.environment.gov.au/system/files/resources/1f98a924-5946-404c-9510-d440304280f1/files/emissions-reduction-fund-white-paper_0.pdf.

Australian Government, 2018. National Inventory Report 2016: Volume 2, Commonwealth of Australia, Canberra, available from: http://www.environment.gov.au/system/files/resources/02bcfbd1-38b2-4e7c-88bd-b2b7624051da/files/national-inventory-report-2016-volume-2.pdf.

Barrett, D.J., 2002. Steady state turnover time of carbon in the Australian terrestrial biosphere. Global Biogeochem. Cycles 16 55–51-55-21.

Berry, S.L., Roderick, M.L., 2006. Changing Australian vegetation from 1788 to 1988: effects of CO2 and land-use change. Aust. J. Bot. 54, 325–338.

Bivand, R., Keitt, T., Rowlingson, B., 2016. rgdal: Bindings for the Geospatial Data Abstraction Library. R package version 1.2-4. https://CRAN.R-project.org/package=rgdal.

Brack, C., Richards, G., Waterworth, R., 2006. Integrated and comprehensive estimation of greenhouse gas emissions from land systems. Sustain. Sci. 1, 91–106.

Breiman, L., 2001. Random forests. Mach. Learn. 45, 5–32.

Cook, G.D., Liedloff, A.C., Cuff, N.J., Brocklehurst, P.S., Williams, R.J., 2015. Stocks and dynamics of carbon in trees across a rainfall gradient in a tropical savanna. Austral Ecol. 40, 845–856.

Dean, C., Wardell-Johnson, G.W., Kirkpatrick, J.B., 2012. Are there any circumstances in which logging primary wet-eucalypt forest will not add to the global carbon burden? Agric. For. Meteorol. 161, 156–169.

Fensham, R.J., Fairfax, R.J., Dwyer, J.M., 2012. Potential aboveground biomass in drought-prone forest used for rangeland pastoralism. Ecol. Appl. 22, 894–908.
Haverd, V., Raupach, M.R., Briggs, P.R., Canadell, J.G., Isaac, P., Pickett-Heaps, C., Roxburgh, S.H., van Gorsel, E., Viscarra Rossel, R.A., Wang, Z., 2013. Multiple observation types reduce uncertainty in Australia's terrestrial carbon and water cycles. Biogeosciences 10, 2011–2040.
Hijmans, R.J., Cameron, S.E., Parra, J.L., Jones, P.G., Jarvis, A., 2005. Very high resolution interpolated climate surfaces for global land areas. Int. J. Climatol. 25, 1965–1978.
Hijmans, R.J., 2016. raster: Geographic Data Analysis and Modeling. R package version 2.5-8. https://CRAN.R-project.org/package=raster.
Jarvis, A., Reuter, H.I., Nelson, A., Guevara, E., 2008. Hole-filled SRTM for the globe Version 4, available from the CGIAR-CSI SRTM 90m Database, http://srtm.csi.cgiar.org.
Keith, H., Mackey, B.G., Lindenmayer, D.B., 2009. Re-evaluation of forest biomass carbon stocks and lessons from the world's most carbon-dense forests. Proc. Natl. Acad. Sci. 106, 11635–11640.
Keith, H., Mackey, B., Berry, S., Lindenmayer, D., Gibbons, P., 2010. Estimating carbon carrying capacity in natural forest ecosystems across heterogeneous landscapes: addressing sources of error. Glob. Change Biol. 16, 2971–2989.
Kesteven, J., Landsburg, J., 2004. Developing a national forest productivity model. National Carbon Accounting System Technical Report No. 23. Commonwealth of Australia.
Kuhn, M., Wing, J., Weston, S., Williams A., Keefer, C., Engelhardt, A., Cooper, T., Mayer, Z., Kenkel, B., the R Core Team, Benesty, M., Lescarbeau, R., Ziem, A., Scrucca, L., Tang, Y., Candan, C., 2016. caret: Classification and Regression Training. R package version 6.0-71. https://CRAN.R-project.org/package=caret Caret R package.
Landsberg, J.J., Waring, R.H., 1997. A generalised model of forest productivity using simplified concepts of radiation-use efficiency, carbon balance and partitioning. For. Ecol. Manage. 95, 209–228.
Lin, L.I.-K., 2000. A note on the concordance correlation coefficient. Biometrics 56, 324–325.
Lowson, C., 2008. Estimating Carbon in Direct Seeded Environmental Plantings. PhD Thesis. Fenner School of Environment and Society, Australian National University.
Meinshausen, N., 2006. Quantile regression forests. J. Mach. Learn. Res. 7, 983–999.
Meinshausen, N., 2016. quantregForest: Quantile Regression Forests. R package version 1.3-5. https://CRAN.R-project.org/package=quantregForest.
Minasny, B., McBratney, A.B., 2006. A conditioned Latin hypercube method for sampling in the presence of ancillary information. Comput. Geosci. 32, 1378–1388.
Montagu, K.D., Cowie, A.L., Rawson, A., Wilson, B.R., George, B.H., 2003. Carbon Sequestration Predictor for land use change in inland areas of New South Wales – background, user notes, assumptions and preliminary model testing. State Forests NSW Research and Development Division Technical Paper No. 68.
Nash, J.E., Sutcliffe, J.V., 1970. River flow forecasting through conceptual models part I—a discussion of principles. J. Hydrol. 10, 282–290.
NVIS, 2016. Pre-1750 Major Vegetation Subgroups - NVIS Version 4.2 (Albers 100m analysis product). http://www.environment.gov.au/fed/catalog/search/resource/details.page?uuid=%7BC665778E-BF5B-4883-AB27-B91DBCE78F9E%7D.
Paul, K.I., Roxburgh, S.H., de Ligt, R., Ritson, P., Brooksbank, K., Peck, A., Wildy, D.T., Mendham, D., Bennett, R., Bartle, J., Larmour, J.S., Raison, R.J., England, J.R., Clifford, D., 2015a. Estimating temporal changes in carbon sequestration in plantings of mallee eucalypts: modelling improvements. For. Ecol. Manage. 335, 166–175.
Paul, K.I., Roxburgh, S.H., England, J.R., de Ligt, R., Larmour, J.S., Brooksbank, K., Murphy, S., Ritson, P., Hobbs, T., Lewis, T., Preece, N.D., Cunningham, S.C., Read, Z., Clifford, D., John Raison, R., 2015b. Improved models for estimating temporal changes in carbon sequestration in above-ground biomass of mixed-species environmental plantings. For. Ecol. Manage. 338, 208–218.
Preece, N.D., Crowley, G.M., Lawes, M.J., van Oosterzee, P., 2012. Comparing above-ground biomass among forest types in the Wet Tropics: small stems and plantation types matter in carbon accounting. For. Ecol. Manage. 264, 228–237.
Raison, R.J., Keith, H., Barrett, D., Burrows, W., Grierson, P.F., 2003. Spatial Estimates of Biomass in 'Mature' Native Vegetation. National Carbon Accounting System Technical Report 44, Australian Greenhouse Office, Canberra, Australia.
Raupach, M.R., Kirby, J.M., Barrett, D.J., Briggs, P.R., Lu H., Zhang L.Z., 2001. Balances of water, carbon, nitrogen and phosphorus in Australian landscapes: (1) model formulation and testing. Technical report 40 / 01. CSIRO Land and Water, Canberra, ACT.
Richards, G.P., 2001. The FullCAM Carbon Accounting Model: Development, Calibration and Implementation for the National Carbon Accounting System. National Carbon Accounting System. Technical Report No. 28. Canberra, Australia.
Richards, G.P., Brack, C., 2004. A continental stock and stock change estimation approach for Australia. Aust. Forest. 67, 284–288.
Richards, G.P., Evans, D.M.W., 2004. Development of a carbon accounting model (FullCAM Vers. 1.0) for the Australian continent. Aust. Forest. 67, 277–283.
Roxburgh, S.H., England, J.R., Paul, K.I., 2010. Developing capability to predict biomass carbon in biodiverse plantings and native forest ecosystems. Client report for Victorian the Government. p. 53.
Roudier, P., 2011. clhs: a R package for conditioned Latin hypercube sampling.
R Core Development Team, 2016. R: A language and environment for statistical computing. R Foundation for Statistical Computing, Vienna, Austria. http://www.Rproject.org/.
Sillett, S.C., Van Pelt, R., Kramer, R.D., Carroll, A.L., Koch, G.W., 2015. Biomass and growth potential of Eucalyptus regnans up to 100 m tall. For. Ecol. Manage. 348, 78–91.
Viscarra Rossel, R.A., Webster, R., Bui, E.N., Baldock, J.A., 2014. Baseline map of organic carbon in Australian soil to support national carbon accounting and monitoring under climate change. Glob. Change Biol. 20, 2953–2970. https://doi.org/10.1111/gcb.12569.
Volkova, L., Roxburgh, S.H., Weston, C.J., Benyon, R.G., Sullivan, A.L., Polglase, P.J., 2018. Importance of disturbance history on net primary productivity in the world's most productive forests and implications for the global carbon cycle. Glob. Change Biol. 24, 4293–4303.
Waterworth, R.M., Richards, G.P., Brack, C.L., Evans, D.M.W., 2007. A generalised hybrid process-empirical model for predicting plantation forest growth. For. Ecol. Manage. 238, 231–243.
Wood, S., Cowie, A., Grieve, A., 2008. Carbon Trading and Catchment Management Authorities: Predicting above-ground carbon storage of plantations. RIRDC Publication No 08/191 RIRDC Project No CGA-2A.